

# Structure-Based Design, Synthesis, and Characterization of Inhibitors of Human and *Plasmodium falciparum* Dihydroorotate Dehydrogenases<sup>†</sup>

Matthew Davies,<sup>‡</sup> Timo Heikkilä,<sup>‡</sup> Glenn A. McConkey, Colin W. G. Fishwick,\* Mark R. Parsons,\* and A. Peter Johnson\*

School of Chemistry, Faculty of Biological Sciences, and Astbury Centre for Structural Molecular Biology, University of Leeds, Leeds LS2 9JT, U.K.

Received July 30, 2008

Pyrimidine biosynthesis is an attractive drug target in a variety of organisms, including humans and the malaria parasite *Plasmodium falciparum*. Dihydroorotate dehydrogenase, an enzyme catalyzing the only redox reaction of the pyrimidine biosynthesis pathway, is a well-characterized target for chemotherapeutical intervention. In this study, we have applied SPROUT-LeadOpt, a software package for structure-based drug discovery and lead optimization, to improve the binding of the active metabolite of the anti-inflammatory drug leflunomide to the target cavities of the *P. falciparum* and human dihydroorotate dehydrogenases. Following synthesis of a library of compounds based upon the SPROUT-optimized molecular scaffolds, a series of inhibitors generally showing good inhibitory activity was obtained, in keeping with the SPROUT-LeadOpt predictions. Furthermore, cocrystal structures of five of these SPROUT-designed inhibitors bound in the ubiquinone binding cavity of the human dihydroorotate dehydrogenase are also analyzed.

## Introduction

The dihydroorotate dehydrogenases (DHODHs) are attractive chemotherapeutic targets in various pathogens, such as *Plasmodium falciparum* and *Helicobacter pylori*, and for the treatment of human disease.<sup>1–3</sup> DHODH catalyzes the conversion of dihydroorotate (DHO) to orotate by utilizing an FMN cofactor in the only redox reaction present in the pyrimidine biosynthesis pathway. The human DHODH (HsDHODH)<sup>a</sup> and the *P. falciparum* DHODH (PfDHODH) both belong to the group of class 2 DHODHs that use respiratory quinones as the terminal electron acceptors. This contrasts with the class 1 enzymes which utilize fumarate or NAD as a cofactor.<sup>4</sup> The class 2 enzymes are membrane-associated and, in eukaryotes, are localized to the inner mitochondrial membrane.<sup>5,6</sup> Kinetic studies have shown a two-site ping-pong mechanism for the conversion of dihydroorotate in class 2 DHODHs.<sup>4,5</sup> Structurally, these enzymes consist of a conserved  $\alpha/\beta$  barrel core and an N-terminal extension, which folds into a separate  $\alpha$ -helical domain.<sup>7–9</sup> Additionally, in eukaryotic organisms, the N-terminal domain extends into the membrane forming a single membrane-anchoring helix, although this is usually truncated for in vitro studies of the enzyme.<sup>10,11</sup> The first half-reaction catalyzed by the enzyme takes place within the core of the protein and comprises the reduction of dihydroorotate to orotic acid with concomitant oxidation of the FMN cofactor. This reaction is mediated by a conserved serine acting as the active site base.<sup>7,10</sup> FMNH<sub>2</sub> is subsequently regenerated by respiratory quinones which, in eukaryotes, are recruited from the inner mitochondrial membrane and are thought to bind to the helical N-terminal domain.

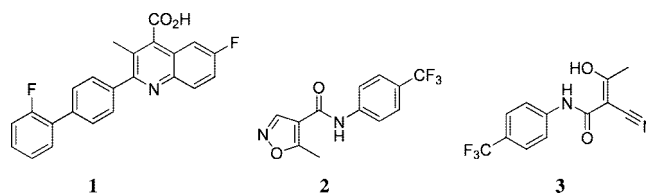


**Figure 1.** Brequinar **1**, leflunomide **2**, and **3** (A77 1726), the active metabolite of leflunomide.

All potent inhibitors of HsDHODH published to date bind to the putative ubiquinone binding channel and display beneficial immunosuppressive and antiproliferative activities, shown to be most pronounced during T-cell proliferation.<sup>11</sup> Brequinar **1** and leflunomide **2** are two examples of low-molecular weight inhibitors of DHODH that have been in clinical development (Figure 1).<sup>11–13</sup> Leflunomide is now marketed as a treatment for rheumatoid arthritis.

Additionally, a group of cyclopentene carboxylic acid amides are in development as HsDHODH-targeting immunosuppressive agents.<sup>14–16</sup> The structure of HsDHODH has been previously determined in complex with compound **3** (the active metabolite of leflunomide), compound **1**, and some of the cyclopentene carboxylic acid amides.<sup>16,17</sup> Inspection of these structures reveals that whereas **1** and **3** both appear to show a single mode of binding to DHODH, a number of the cyclopentene carboxylic acid amides display an interesting dual binding mode within the same cocrystal.

The structure of **3** cocrystallized with the *P. falciparum* DHODH has been reported recently.<sup>8</sup> Although this compound is a relatively weak inhibitor of the *Plasmodium* enzyme, this system provides a good starting point for structure-based development of more potent inhibitors. The binding mode observed for **3** in the PfDHODH cocrystal structure differs significantly from that observed in the HsDHODH cocrystal structure (Figure 2). In the PfDHODH–**3** complex, three direct hydrogen bonds can be observed (to His185, Arg265, and Tyr528), whereas in the HsDHODH–**3** complex, there are water-mediated hydrogen bonds to Arg265 and Gln47 in addition to the direct hydrogen bond to Tyr356. Closer inspection of the binding cavities also shows that in both cases, the

<sup>†</sup> Crystal structural coordinates are deposited in the Protein Data Bank as entries 3FIQ, 3FJ6, 3FJL, 3G0U, and 3GOX.

\* To whom correspondence should be addressed. C.W.G.F.: e-mail, c.w.g.fishwick@leeds.ac.uk; phone, +44 113 3436510; fax, +44 113 3436530. M.R.P.: e-mail, m.r.parsons@leeds.ac.uk; phone, +44 113 3432574; fax, +44 113 3433106. A.P.J.: e-mail, p.johnson@leeds.ac.uk; phone, +44 113 3436515; fax, +44 113 3436530.

<sup>‡</sup> These authors contributed equally to this work.

<sup>a</sup> Abbreviations: PfDHODH, *P. falciparum* dihydroorotate dehydrogenase; HsDHODH, human dihydroorotate dehydrogenase; DHO, dihydroorotate; CoQ, ubiquinone coenzyme; FMN, flavin mononucleotide.

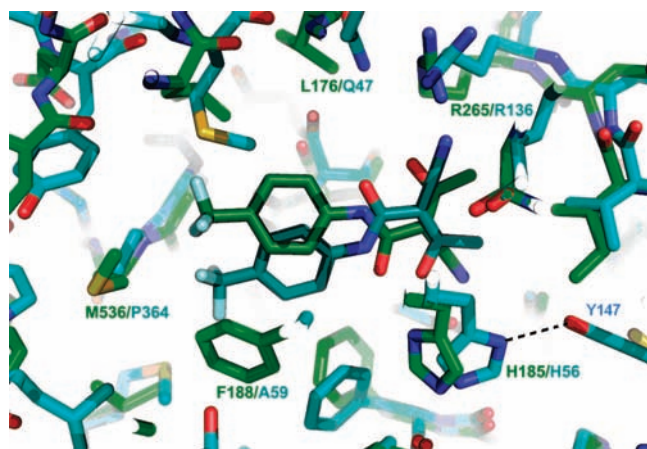


**Figure 2.** Overlay of **3** bound in HsDHODH (blue) and PfDHODH (green), illustrating the different binding mode of the inhibitor in each case. Note that the “headgroup” of the inhibitor adopts an opposite orientation. In PfDHODH, hydrogen bonds are made to His185, Arg265, and Tyr528, whereas in HsDHODH, hydrogen bonds are formed to Gln47/Arg136 (water-mediated) and to Tyr356 and, significantly, a hydrogen bond to Tyr147 holds His56 in a conformation where hydrogen bonding to **3** is no longer possible.

trifluoromethyl phenyl section of the inhibitor only partly fills a portion of the binding cavity that is mainly lined by hydrophobic amino acid residues. In the case of the compound **3**-derived cocrystal structures, the presence of this unoccupied space holds promise in the design of suitable variants of these inhibitors which would better fill this cavity. In addition to the likely increase in binding affinities, inhibitors designed to more effectively fill the binding cavities could also exploit differences in the shapes between the two cavities, possibly leading to species-specific selectivity. Because of the existence of the salvage pathway in humans, such selectivity may not be essential for the development of new antiplasmodial agents targeting PfDHODH. Of course, such selectivity is highly desirable, particularly since leflunomide, the pro-drug precursor of compound **3**, has been found to exhibit some dose-dependent side effects in a small number of patients.<sup>18</sup>

Here, we present the results of a computational structure-based lead optimization exercise aimed at improving the binding of compound **3** to the ubiquinone binding cavities in DHODH. A small number of compounds were synthesized and tested against the human and *P. falciparum* enzymes in inhibition assays. We observed that a number of the compounds were very potent inhibitors of the human DHODH, and therefore, the cocrystal structures of five of the most potent compounds bound to the ubiquinone binding site of HsDHODH were determined and analyzed.

## Results and Discussion

**Lead Optimization and Analysis of Inhibitors.** Structure-based computational molecular design is an important tool for use in medicinal chemistry and chemical biology, and such methods have been recognized as offering considerable potential when applied to early stage drug discovery. In particular, the importance of these methods in therapeutic areas where random high-throughput screening has proved disappointing, such as in the discovery of new anti-infective agents, has been recently underlined.<sup>19</sup> We have previously described the application of the de novo molecular design program SPROUT to the production of a number of enzyme inhibitors and receptor antagonists.<sup>20</sup> SPROUT is a program that uses a fragment-based approach applied to a targeted cavity (e.g., active site) within

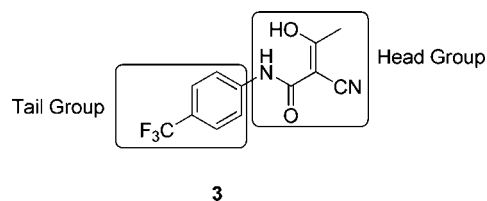


**Figure 3.** Hydrophobic tail moiety and hydrogen bond-forming headgroup of inhibitor **3**.

the X-ray crystal structure of the chosen protein to construct putative ligand scaffolds. The system can then be used to rank these designed scaffolds using various considerations such as predicted binding affinity and molecular complexity to aid in the choice of compound for synthesis. Very recently, we have developed a variant of this software, SPROUT-LeadOpt, which can take the structure of a small molecule complexed to a protein (e.g., a cocrystallized enzyme inhibitor) and generate variants predicted to have higher affinities. A particular feature of this software is that the generation of the variant structures is performed using a retrosynthetic approach utilizing a chemistry knowledge base and a library of commercially available starting materials from which alternative “monomers” (which are structural variants of the monomers found in the original structure) are automatically selected.

As part of an ongoing program aimed at the development of inhibitors of class 2 DHODHs using structure-based methods,<sup>21</sup> we wished to utilize SPROUT-LeadOpt to rationally improve the binding affinity of inhibitor **3** that has been previously cocrystallized with both the human and *Plasmodium* DHODH enzymes. In this study, we set out to generate simple compounds that would utilize the hydrogen bonding network from the headgroup moiety of compound **3** and have an improved “tail” (Figure 3) that fills the hydrophobic pocket at the entrance to the binding cavity.

In addition to the partially filled hydrophobic cavity occupied by the tail section of inhibitor **3**, further analysis of the ligand binding cavities of both cocrystal structures using SPROUT revealed the presence of a second, smaller hydrophobic cavity in the region occupied by the methyl group within the head section of the inhibitor. As this cavity again appeared to be only partially occupied, we began by investigating the effect of replacing the methyl moiety with a number of larger hydrophobic groups to fit into the pocket at the end of the ubiquinone binding channel (Table 1, compounds **4–9**). The tail of compound **3** was extended by replacement of the CF<sub>3</sub> group by a phenyl ring to give a biphenyl tail (Table 1, compounds **10–16**). The biphenyl tail was incorporated into the inhibitors to improve their binding through enhanced hydrophobic interactions within the large hydrophobic region of the PfDHODH binding cavity.

Following enzymatic screening of compounds **4–16** (see the Supporting Information) with both the human and *Plasmodium* DHODH enzymes, it was evident that substitution of the methyl group in compound **3** for a cyclopropyl group as in **4** led to an increase in binding affinity for both *Plasmodium* and human DHODH (Table 2), consistent with previous observations for the rodent enzymes.<sup>22</sup> However, further increases in the size of the hydrophobic substituents at this position (as in compounds **5–9**) resulted in an adverse effect upon inhibition of enzymatic activity compared to that of compound **3** itself (results not shown). Furthermore, replacement of the trifluoromethyl group in compound **3** with phenyl as in **10** resulted in a significant improvement in binding affinities for both of the enzymes

**Table 1.** Analogues of Compound 3

Compound	R <sup>1</sup>	R <sup>2</sup>	Compound	R <sup>1</sup>	R <sup>2</sup>
<b>4</b>		CF <sub>3</sub>	<b>10</b>	CH <sub>3</sub>	
<b>5</b>		CF <sub>3</sub>	<b>11</b>		
<b>6</b>		CF <sub>3</sub>	<b>12</b>		
<b>7</b>		CF <sub>3</sub>	<b>13</b>		
<b>8</b>		CF <sub>3</sub>	<b>14</b>		
<b>9</b>		CF <sub>3</sub>	<b>15</b>		
			<b>16</b>		

**Table 2.** Experimentally Defined IC<sub>50</sub> and K<sub>i</sub><sup>app</sup> Values for Compound 3 and Derivatives<sup>a</sup>

Inhibitor	PfDHODH IC <sub>50</sub>	PfDHODH K <sub>i</sub> <sup>app</sup>	HsDHODH IC <sub>50</sub>	HsDHODH K <sub>i</sub> <sup>app</sup>
	190.1 μM	22 μM	0.261 μM	0.032 μM
<b>3</b>				
	92.5 μM	11 μM	0.117 μM	0.014 μM
<b>4</b>				
	25.7 μM	3.0 μM	0.090 μM	0.011 μM
<b>10</b>				
	223.6 μM	26 μM	0.053 μM	0.007 μM
<b>11</b>				

<sup>a</sup> For the complete data set of biological activity of compounds 4–16, see the Supporting Information.

studied here (Table 2). A combination of these features, however, as in compound **11** resulted in good inhibition of HsDHODH but an 8-fold reduction in activity against PfDHODH (Table 2).

Inspection of the SPROUT-generated models of inhibitors **4**, **10**, and **11** bound within both the human and *Plasmodium* DHODH crystal structures revealed some important differences in terms of the requirements for efficient inhibitor binding

between the cavities for both enzymes. For instance, inhibitor **4**, containing a cyclopropyl-based headgroup, is predicted to fit comfortably into the binding channels of both enzymes. In the case of inhibitor **10**, however, modeling indicated that acceptable binding within the *Plasmodium* enzyme to maintain the predicted H-bonding to the residues in the headgroup region required movement of the side chain of Met536 which lies toward the entrance of the binding cavity (Figure 4). Even if

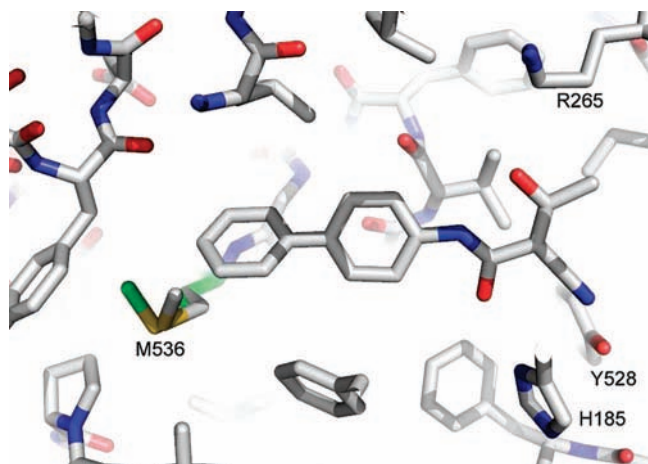


**Figure 4.** Movement of the side chain of Met536 (gray, before; green, after) required for the binding of **10** in PfDHODH.

we allow for this movement, the *S*-methyl group forming part of the Met536 side chain is predicted to make unfavorable steric interactions with the phenyl group of inhibitor **10** which appears to be reflected in the rather modest inhibition observed for PfDHODH (Table 2). In the case of HsDHODH, where Met536 is replaced with Pro364, the shape of the cavity is such that inhibitor **10** is predicted to fit comfortably in the binding cavity, consistent with the good observed inhibition of HsDHODH.

Additionally, analysis of the modeled complex of inhibitor **10** and PfDHODH revealed the existence of a number of discrete subcavities and clefts in the protein surface surrounding the large hydrophobic tunnel containing the biphenyl tail of the inhibitor. To further increase inhibitor affinity, SPROUT-LeadOpt was used to identify substituted biaryl-based variants of inhibitor **10** that were predicted to maximize binding of the inhibitor within the hydrophobic tunnel. SPROUT-LeadOpt's automated retrosynthetic analysis of **10** yielded phenylboronic acid and 4-bromoaniline as commercially available monomers. Automatic substitution of fragments derived from commercially available superstructure compounds followed by redocking and scoring gave a series of alternative monomers. This resulted in the design of a range of mono- and disubstituted biaryl-based systems [compounds **17–29** (Table 3)] which were predicted (SPROUT score) to bind with greater affinity to PfDHODH compared to compound **3** or the biphenyl **10**. Following synthesis (see below), these systems were assayed with both the *Plasmodium* and human DHODH enzymes. In all but one case (compound **25**), these compounds were found to display a stronger inhibition of PfDHODH compared to that found for compound **3**, in keeping with the modeling predictions. Additionally, compounds **17–21** showed increased inhibitory activity with PfDHODH compared to that of inhibitor **10** (Table 3). Almost all of these biaryls exhibited greater inhibitory action toward HsDHODH than PfDHODH, the exceptions being compounds **21** and **23** which displayed a marginal inhibitory preference for the *Plasmodium* enzyme (Table 3). However, it is noteworthy that in contrast to the behavior of these inhibitors with PfDHODH, the introduction of substituents into the biphenyl tail of compound **10** produced compounds that generally had reduced potency for the human enzyme. We have recently reported<sup>21</sup> a series of anthranilic acid analogues that were potent PfDHODH inhibitors, and because of the relative shapes of the binding cavities in both enzymes, it was found that those inhibitors with structures able to exist in a nonplanar conformation were shown to display greater affinity for the parasite enzyme over the human enzyme. In light of these earlier observations, it was expected

that this effect would be most pronounced in the case of compound **21** where the doubly ortho-substituted benzene ring would induce a 90° angle between the two biaryl rings, and indeed, modest selectivity for PfDHODH over the human enzyme was observed (Table 3).

The potential for inhibitors of PfDHODH to act as antiplasmodial agents has recently been underlined<sup>23,24</sup> in high-throughput screening studies which led to the identification of potent and selective inhibitors of this enzyme. Interestingly, preliminary testing of eight compounds (**17–20**, **22**, **23**, **26**, and **28**) against parasites (data not shown) indicated that compounds **17–19** exhibited activity in the micromolar range, indicating that these inhibitors merit further and more detailed investigation into their potential as antiplasmodial agents.

**Structures of Inhibitors in Complex with HsDHODH.** In light of the generally good affinity shown by the inhibitors for the human enzyme, we investigated the details of their interaction with HsDHODH using X-ray crystallography. Cocrystal structures were determined for five potent inhibitors bound to human DHODH. The structures were determined to a high resolution and allow a detailed analysis of the interactions between the enzyme and inhibitors. In general, the protein components of the structures of these five cocrystal complexes are nearly identical to previously published structures of HsDHODH ( $C_{\alpha}$  rmsd < 0.25 Å).<sup>7,17</sup>

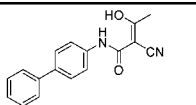
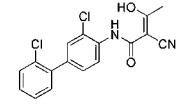
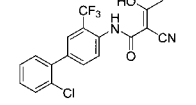
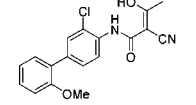
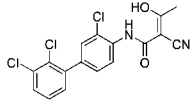
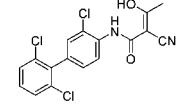
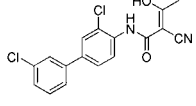
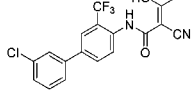
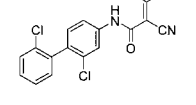
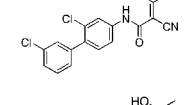
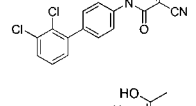
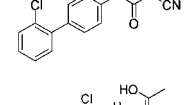
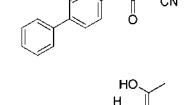
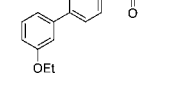
As previously reported, some parts of the structures remain disordered,<sup>7,17</sup> and in particular, the surface loops consisting of residues 69–71 and residues 216–221 are poorly defined in the electron density map. Furthermore, the N-terminal polyhistidine tag and the following linker region are fragmented in density and could not be built into the final model. Analysis of the membrane association domain also reveals density attributable to the detergent molecules between and at the ends of the two  $\alpha$ -helices comprising the N-terminal domain.<sup>7</sup> This density was also quite fragmented, and the detergent molecules were not built into any of the models. As expected, the majority of the differences seen in the side chain conformations appear to be concentrated in the ubiquinone binding channel and are most likely induced by the binding of the inhibitors.

In most cases, the head moiety occupies the same part of the cavity as compound **3**, and the water-mediated hydrogen bonds to Gln47 and Arg136 have been preserved. Additionally, and consistent with the SPROUT-derived models of these complexes, the biphenyl tail extends toward the surface of the protein and fills the hydrophobic region of the target binding cavity. All of the cocrystal structures here clearly show a single mode of binding for the inhibitors (Figure 5).

However, in the HsDHODH–**24** cocrystallized complex, the headgroup moiety of the inhibitor is rotated 180° compared to its orientation in the cocrystal structures of the other inhibitors and that of compound **3** and instead (Figure 6) adopts a conformation similar to that observed for compound **3** in the PfDHODH enzyme. Following the nomenclature established previously,<sup>16</sup> this binding mode can be designated as “non-A77 1726-like”. However, it should be noted that despite this change in the pose adopted by the ligand, and in contrast to the situation with PfDHODH depicted in Figure 3, the conformation adopted by His56 still precludes formation of a hydrogen bond to the ligand, because the alternative hydrogen bond to a water molecule is apparently preferred (Figure 6).

The cocrystal structures of **10**, **19**, and **29** involve two water-mediated hydrogen bonds (to residues Arg136 and Gln47) and a direct hydrogen bond involving the hydroxyl of Tyr356. In the case of **24**, however, although involving similar interactions,

**Table 3.** Experimentally Defined IC<sub>50</sub> and K<sub>i</sub><sup>app</sup> Values for Compounds Developed from **10** Using SPROUT-LeadOpt

Inhibitor	PfDHODH IC <sub>50</sub> (μM)	PfDHODH K <sub>i</sub> <sup>app</sup> (μM)	HsDHODH IC <sub>50</sub> (μM)	HsDHODH K <sub>i</sub> <sup>app</sup> (μM)
<b>10</b> 	25.7	3.0	0.091	0.011
<b>17</b> 	4.0	0.48	0.18	0.022
<b>18</b> 	6.2	0.73	0.17	0.021
<b>19</b> 	8.6	1.0	0.20	0.025
<b>20</b> 	9.9	1.2	0.33	0.040
<b>21</b> 	10.2	1.2	16.5	2.0
<b>22</b> 	49.1	5.8	1.52	0.19
<b>23</b> 	57.2	6.8	86.6	10.7
<b>24</b> 	165.0	20.5	0.022	0.0027
<b>25</b> 	236.6	28.0	0.19	0.023
<b>26</b> 	27.2	3.2	0.20	0.025
<b>27</b> 	47.4	5.6	0.13	0.016
<b>28</b> 	51.1	6.0	0.32	0.039
<b>29</b> 	182.4	21.5	0.13	0.016

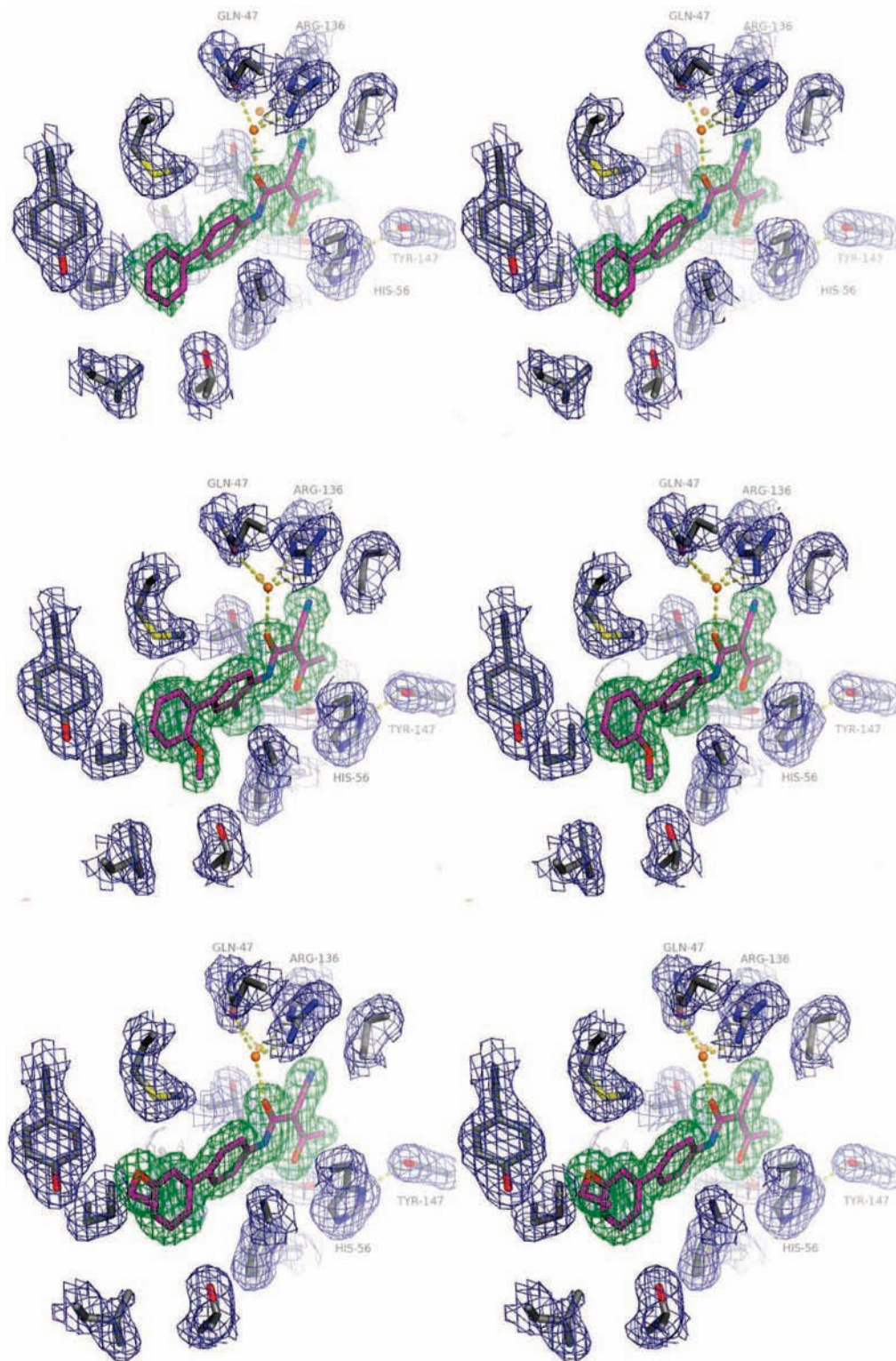


**Figure 5.** Stereo images of the binding modes of compounds **10**, **19**, and **29**. The conserved histidine, His56, appears to form a hydrogen bond with Tyr147, thus locking His56 in a conformation that allows stacking against the headgroup of the inhibitor and prevents H-bonding to the inhibitor. Water molecules are shown as orange spheres. The  $2F_o - F_c$  electron density map is contoured at  $2\sigma$  around the ligand, with the compound built in the difference electron density using COOT (see the Supporting Information for details).

here it is the nitrile that forms a hydrogen bond with Tyr356 while contact to Arg136 remains water-mediated (Figure 6). The torsion angle between the amide moiety and the adjacent aryl ring of the biphenyl is considerably larger in the HsD-HODH-**24** complex than in the complex with the unsubstituted compound, **10** ( $42^\circ$  vs  $20^\circ$ , respectively). This difference in overall molecular shape appears to be closely related to the

difference in the binding modes involving the additional hydrogen bonding interaction of compound **24** with Tyr147. This is then reflected in the binding affinity, as compound **24** is the most potent of the inhibitors studied here, with a  $K_i^{app}$  of 2.7 nM.

Binding of the cyclopropyl-containing compound **11** closely resembles that of **10** and **3**. The cyclopropyl group occupies a

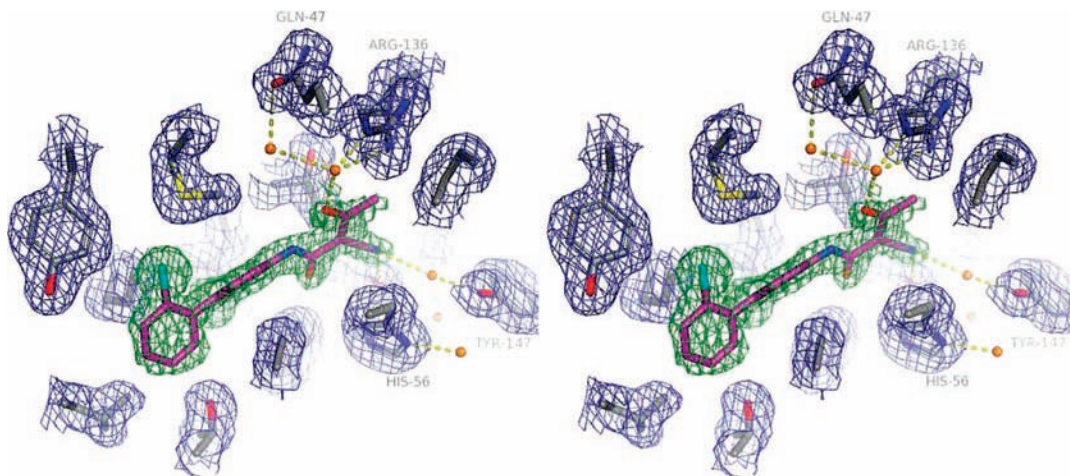


**Figure 6.** Stereo image of compound **24** bound to the ubiquinone binding site of HsDHODH. The binding mode of **24** shows an additional water-mediated hydrogen bond to Tyr147 in addition to the direct hydrogen bond to Tyr356 as well as the water-mediated hydrogen bonds to Gln47 and Arg136. Water molecules are shown as orange spheres. The  $2F_o - F_c$  electron density map is contoured at  $2\sigma$  around the ligand, with the compound built in the difference electron density using COOT.

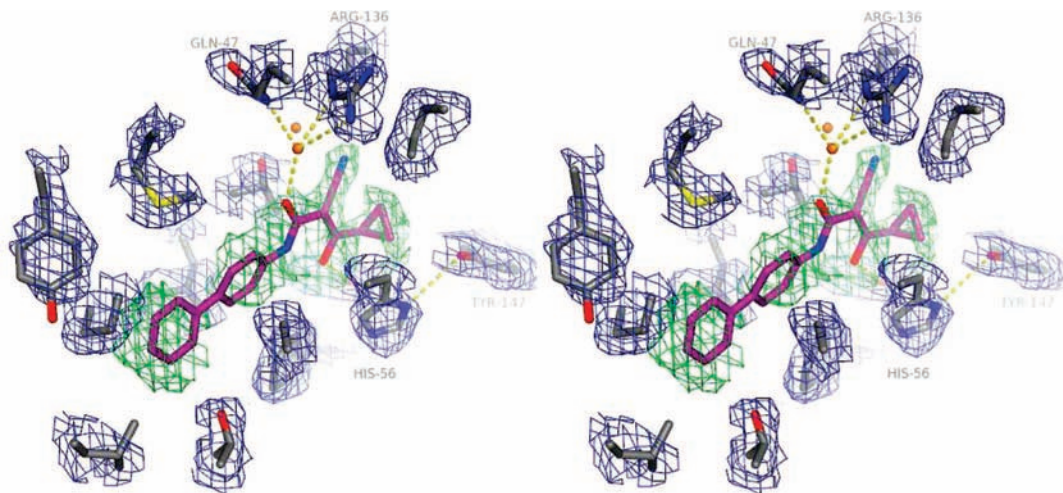


**Figure 7.** Stereo image of compound **11** bound to the ubiquinone binding site of HsDHODH. The compound binds in an A77 1726-like binding mode. Water molecules are shown as orange spheres. The  $2F_o - F_c$  electron density map is contoured at  $1\sigma$  around the ligand, with the compound built in the difference electron density using COOT.

small cavity lined by hydrophobic residues above Tyr356 and next to the FMN (Figure 7).

Detailed examination of the structure of the bound inhibitor within the compound **11**–HsDHODH complex revealed the presence of a conformation in which the cyclopropyl ring is bisected by the adjacent enolic hydroxyl group which is consistent with observations reported previously for similar cyclopropyl-based amides.<sup>25</sup>

Additionally, to accommodate the binding mode of compound **11**, His56 adopts a conformation similar to that found in the cocrystal structures containing compounds **10**, **19**, and **29** (Figure 5) and features an H-bond between His56 and Tyr147.

**Predicted Binding Mode of Inhibitors in PfDHODH.** All compounds that were found to be inhibitors of PfDHODH were predicted, using SPROUT, to bind in a manner similar to that observed for compound **10**, with the planar headgroup making direct hydrogen bonds to residues Arg265, His185, and Tyr528. The biphenyl tail of each inhibitor was predicted to bind in the large hydrophobic region of the binding cavity, in a fashion analogous to that found for these inhibitors in HsDHODH. Furthermore, the substituted biaryl moiety present in these inhibitors was predicted to occupy the binding cavity more

extensively compared to that of compound **10**. The SPROUT-generated structures for two representative examples are shown in Figure 8.

It was predicted that all the inhibitors would bind along the same common axis and make the same hydrogen bonding interactions (Figure 8). Therefore, differences in the ring substituents and their pattern of substitution were predicted to largely dictate the different levels of inhibition of PfDHODH. It is clear from the inhibitory activity observed for compounds **26**–**29**, that substitution in just one of the aromatic rings did not lead to improved inhibitory activity with respect to compound **10**. The combination of substituents in both aromatic rings of the biaryl tail appears to be an important requirement for maximal inhibitor activity with PfDHODH. Compounds **17**–**19** and **21** were all more active (by between 3- and 6-fold) than compound **10** in PfDHODH, and they were the most active of the series. These compounds all feature substituents in the aromatic ring, which contains the cyanohydroxybutenamide moiety, that are ortho to this position of cyanohydroxybutenamide attachment (for convenience, here labeled as ortho) together with substituents in the terminal aromatic ring which

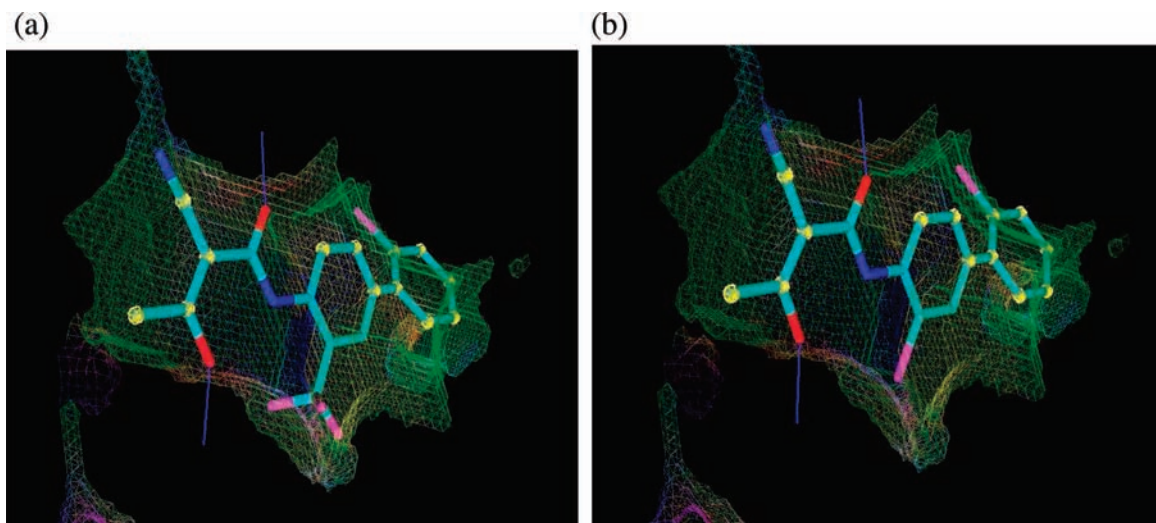


**Figure 8.** SPROUT-generated structures of (a) compound **18** showing the boundary surface of the PfDHODH cavity and (b) compound **17** showing the boundary surface of the PfDHODH cavity.

are ortho-substituted with respect to the aryl attachment (here termed ortho'). Other substitutions are labeled in a similar manner.

As is apparent from Table 3, the biaryl-substituted compounds were generally more active against HsDHODH than PfDHODH. As an example, compound **29** is more than 1000 times more active against HsDHODH than PfDHODH. As previously noted,<sup>8</sup> in the PfDHODH crystal structure, the opening to the binding cavity is relatively narrow because of the presence of Met536, which may act to hinder entry of inhibitors such as compound **29**. However, in the human enzyme, the opening to the binding cavity is wider than for PfDHODH and therefore appears to facilitate entry of inhibitors.

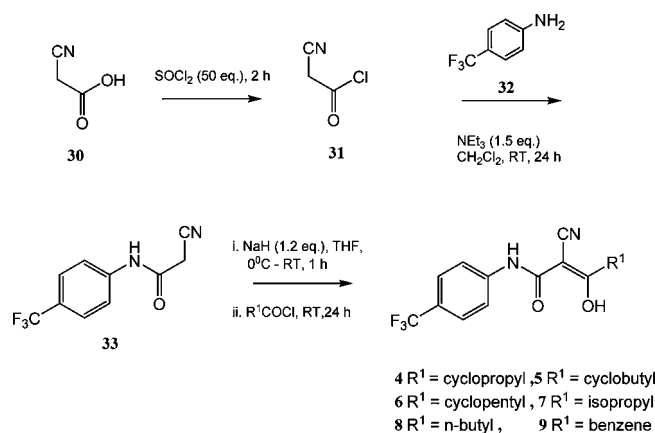
Interestingly, as a further illustration of the importance of molecular shape in enzyme selectivity, compound **21** was found to be approximately 2-fold more selective for PfDHODH than for HsDHODH. This appears to reflect the tendency for the di-ortho'-substituted benzene ring present in **21** to maximize the dihedral angle between the aromatic rings of the biphenyl tail, resulting in a rather cylindrical-shaped molecule which would appear to better occupy the cylindrical-like cavity in PfDHODH as opposed to the somewhat flattened cavity in the human enzyme. However, it seems likely that in those cases where excellent selectivity is observed,<sup>23,24,26</sup> this is due to strong hydrogen bonding interactions to the residues in the headgroup region of PfDHODH. As noted in Figure 5, one very significant difference between PfDHODH and HsDHODH in this region is that in HsDHODH, His56 is hydrogen bonded to Tyr147 and hence is not readily available for hydrogen bonding to ligands. This is also true for all the structures reported in this study. We suggest that for PfDHODH, formation of a strong hydrogen bond between a ligand and His185 might well be a requirement for inhibitors to be highly selective for PfDHODH versus HsDHODH. Some evidence for this hypothesis comes from mutagenesis studies<sup>26–28</sup> which show that mutation of His185 in PfDHODH leads to a very significant loss of inhibitory activity (500–1000-fold increase in IC<sub>50</sub>) for some highly selective inhibitors.

## Chemistry

Compounds **4–9** were prepared using the route shown in Scheme 1.<sup>22</sup>

Treatment of acid chloride **31** (obtained from cyanoacetic acid **30** and used without purification) with *p*-trifluoromethylaniline **32**

## Scheme 1



gave intermediate cyanoacetamide **33** in 57% yield, which was then treated with sodium hydride followed by the appropriate acyl halide (R<sup>1</sup>COCl) yielding the target compounds (60–79%).

The biphenyl **10** was synthesized according to the route shown in Scheme 2.

Curtius rearrangement of acyl azide **35** (obtained from *p*-biphenylcarboxylic acid **34**) gave isocyanate **36**, which was treated immediately and without further purification with the sodium salt of cyanoacetone **37** to give compound **10** in 81% yield.

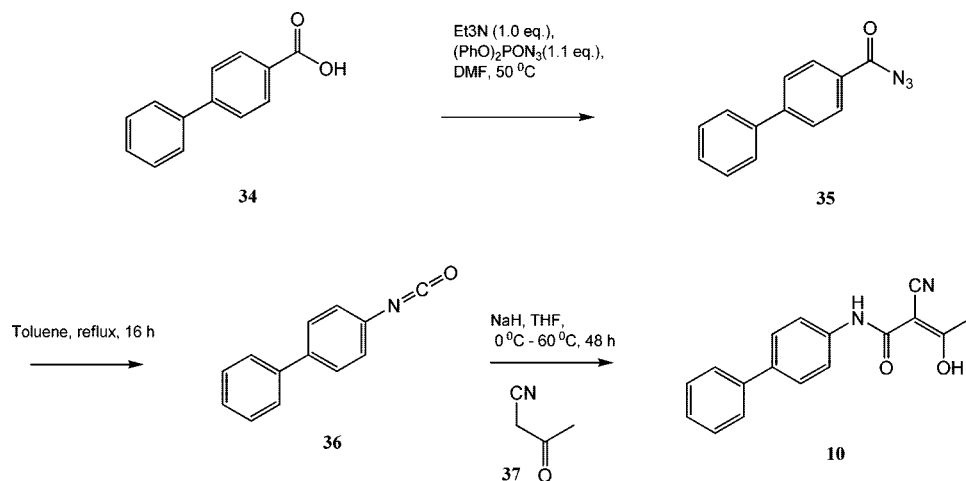
For the synthesis of compounds **11–16**, treatment of cyanoacetamide **38** with sodium hydride in THF followed by addition of the appropriate acid chloride (R<sup>1</sup>COCl) afforded the target compound (Scheme 3).

Compounds **17–29** were synthesized according to the general scheme in Scheme 4.

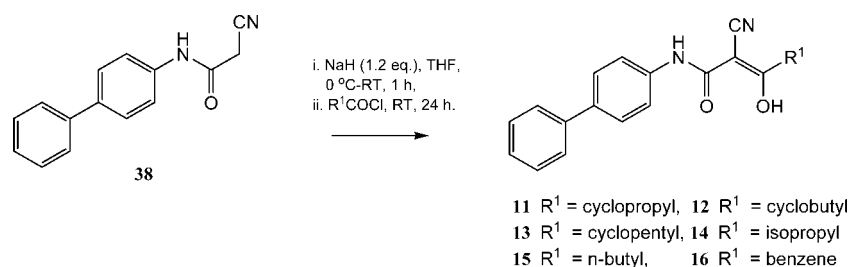
In step A, substituted biphenylanilines were obtained via Suzuki coupling of the appropriate substituted boronic acids **39** with substituted 4-bromoanilines **40** using catalytic quantities of Pd(OAc)<sub>2</sub> and PPh<sub>3</sub> in refluxing toluene for 24 h. The reaction could also be carried out by stirring the reagents under microwave irradiation at 160 °C for 40 min. Performing these Suzuki couplings on a millimole scale under conditions of microwave irradiation was advantageous over conventional heating due to reduced reaction times; however, the microwave instrument was not amenable to larger-scale reactions, and reaction conducted under standard reflux conditions was the preferred method. The yields of products (compounds **41a–41i**; see the experimental section in the Supporting Information) were similar using either method and were in the range of 33–100%, with the exception being compound **41b**



## Scheme 2



## Scheme 3



## Scheme 4

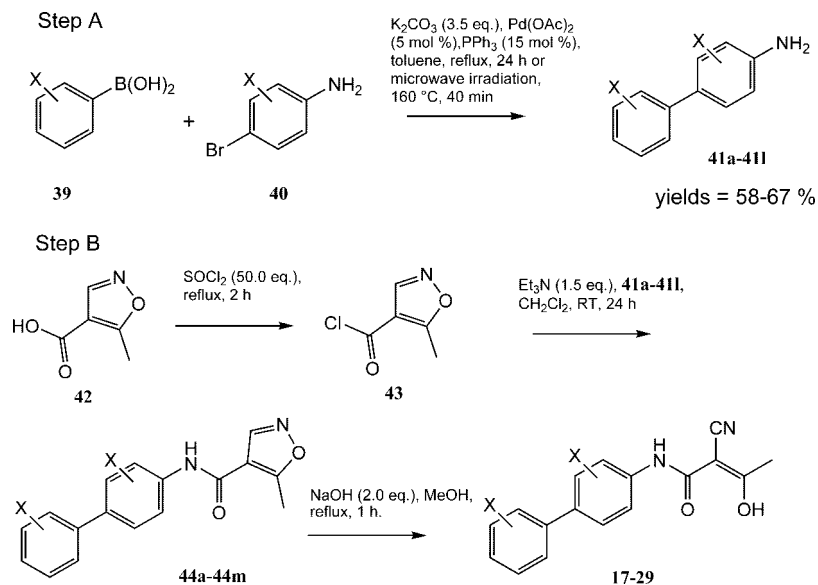
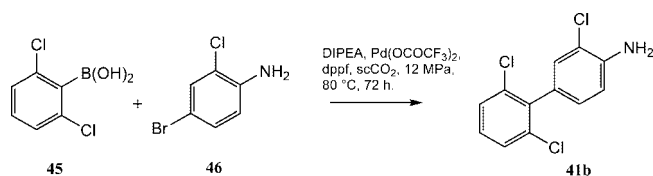


(Figure 9), obtained in only 3% yield. Other conditions were then explored to improve the yield of compound **41b** (see the next section). In step B, 5-methylisoxazole-4-carboxylic acid **42** was treated with thionyl chloride to give acid chloride **43**, which was then treated with the appropriate substituted aminobiphenyl (**41a–41l**) to yield the corresponding amides in yields of 70–85%. The O–N bond of the isoxazole moiety was then cleaved via treatment with NaOH to afford the SPROUT-LeadOpt-designed compounds in generally excellent yields (90–100%).

**Synthesis of Compound 41b.** A range of conditions were explored for the synthesis of compound **41b**, and the best results were obtained using supercritical (sc) CO<sub>2</sub> (Scheme 5).

## Scheme 5



We suspected that the steric hindrance around the boron atom in boronic acid **45** was giving rise to the poor yields observed in the Suzuki coupling reactions of **45** with **46**. Additionally, we reasoned that for this case, there could be a competing process

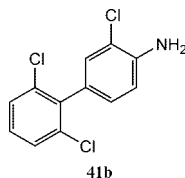


**Figure 9.** Trichloro-substituted biphenylaniline obtained in only 3% yield using conventional Suzuki coupling conditions.

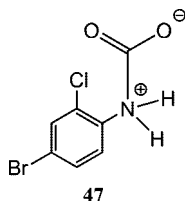


**Figure 10.** Proposed N-carboxylated intermediate **47** from 4-bromo-2-chloroaniline **46** and carbon dioxide.

involving coordination of aniline **46** to the palladium catalyst, thereby resulting in “catalyst poisoning” and further reducing the efficiency of the reaction. When a mixture of **45** and **46** along with diisopropylethylamine, 1,1'-bis(biphenylphosphino)ferrocene, and palladium bistrifluoroacetate was stirred in  $scCO_2$  under pressure (12 MPa) at 80 °C over a period of 72 h, compound **41b** was obtained in 51% yield. However, when the equivalent reaction was conducted in toluene, only starting materials were recovered from the reaction mixture. In the presence of  $scCO_2$ , it is proposed that an N-carboxylated intermediate **47** is likely formed from aniline **46**, thus preventing deactivation of the palladium catalyst via amine coordination (Figure 10). Additionally as previously reported,<sup>29</sup> the use of  $scCO_2$  may enhance the stability of the palladium catalyst and prevent decomposition.

## Conclusions

We have applied the computer-aided molecular design program SPROUT-LeadOpt to cocrystal structures of an existing inhibitor in both human and *Plasmodium* DHODH. On the basis of the resulting designed molecular scaffolds, a small library of compounds was prepared and these molecules were screened against both human and *Plasmodium* enzymes. Essentially all of the designed inhibitors exhibited enhanced levels of inhibition for both the *Plasmodium* and human DHODH enzymes compared to that observed for the existing inhibitor **3**. The majority of inhibitors were selective for HsDHODH which may indicate that variations in the hydrophobic tail of these ligands can at best (**21** and **23**) give modest selectivity for PfDHODH versus HsDHODH, perhaps by exploiting differences between the hydrophobic surfaces of the proteins in this region. It is argued that many (but not necessarily all) highly selective inhibitors will exploit the possibility of a strong hydrogen bond to His185 in PfDHODH which is much more difficult for the corresponding His56 in HsDHODH, because it would involve loss of an intramolecular hydrogen bond to Tyr147. Additionally, several X-ray cocrystal structures of the inhibitors in complex with HsDHODH have been determined to a high resolution. The detailed molecular interactions apparent within these structures were generally in good agreement with those derived from the design of these structures using SPROUT-LeadOpt.

**Acknowledgment.** We gratefully acknowledge the support of the EPSRC (studentship to M.D.) and the Wellcome Trust (studentship to T.H.).

**Supporting Information Available:** A table listing the degree of purity for all target compounds (area percent and retention time),

a table listing the elemental analyses, details of the experimental procedures, and spectroscopic data for each compound, details of the biological assays, and details of protein crystallography. This material is available free of charge via the Internet at <http://pubs.acs.org>.

## References

- (1) Tamta, H.; Mukhopadhyay, A. K. Biochemical targets for malaria chemotherapy. *Current Research & Information on Pharmaceutical Science (CRIPS)* **2003**, *4*, 6–9.
- (2) Copeland, R. A.; Marcinkeviciene, J.; Haque, T. S.; Kopcho, L. M.; Jiang, W.; Wang, K.; Ecret, L. D.; Sizemore, C.; Amsler, K. A.; Foster, L.; Tadesse, S.; Combs, A. P.; Stern, A. M.; Trainor, G. L.; Slee, A.; Rogers, M. J.; Hobbs, F. *Helicobacter pylori*-selective antibacterials based on inhibition of pyrimidine biosynthesis. *J. Biol. Chem.* **2000**, *275*, 33373–33378.
- (3) Morand, P.; Courtin, O.; Sautes, C.; Westwood, R.; Hercend, T.; Kuo, E. A.; Ruuth, E. Dihydroorotate dehydrogenase is a target for the biological effects of leflunomide. *Transplant. Proc.* **1996**, *28*, 3088–3091.
- (4) Palfey, B. A.; Bjornberg, O.; Jensen, K. F. Insight into the chemistry of flavin reduction and oxidation in *Escherichia coli* dihydroorotate dehydrogenase obtained by rapid reaction studies. *Biochemistry* **2001**, *40*, 4381–43290.
- (5) Norager, S.; Jensen, K. F.; Bjornberg, O.; Larsen, S. *E. coli* dihydroorotate dehydrogenase reveals structural and functional distinctions between different classes of dihydroorotate dehydrogenases. *Structure* **2002**, *10*, 1211–1223.
- (6) Krungkrai, J. Purification, characterization and localization of mitochondrial dihydroorotate dehydrogenase in *Plasmodium falciparum*, human malaria parasite. *Biochim. Biophys. Acta* **1995**, *1243*, 351–360.
- (7) Liu, S.; Neidhardt, E. A.; Grossman, T. H.; Ocain, T.; Clardy, J. Structures of human dihydroorotate dehydrogenase in complex with antiproliferative agents. *Structure* **2000**, *8*, 25–33.
- (8) Hurt, D. E.; Widom, J.; Clardy, J. Structure of *Plasmodium falciparum* dihydroorotate dehydrogenase with a bound inhibitor. *Acta Crystallogr.* **2006**, *D62*, 312–323.
- (9) Loffler, M.; Knecht, W.; Rawls, J.; Ullrich, A.; Dietz, C. *Drosophila melanogaster* dihydroorotate dehydrogenase: The N-terminus is important for biological function in vivo but not for catalytic properties in vitro. *Insect Biochem. Mol. Biol.* **2002**, *32*, 1159–1169.
- (10) Hansen, M.; Le Nours, J.; Johansson, E.; Antal, T.; Ullrich, A.; Loffler, M.; Larsen, S. Inhibitor binding in a class 2 dihydroorotate dehydrogenase causes variations in the membrane-associated N-terminal domain. *Protein Sci.* **2004**, *13*, 1031–1042.
- (11) McLean, J. E.; Neidhardt, E. A.; Grossman, T. H.; Hedstrom, L. Multiple inhibitor analysis of the Brequinar and leflunomide binding sites on human dihydroorotate dehydrogenase. *Biochemistry* **2001**, *40*, 2194–2200.
- (12) Fox, R. I.; Herrmann, M. L.; Frangou, C. G.; Wahl, G. M.; Morris, R. E.; Strand, V.; Kirschbaum, B. J. Mechanism of action for leflunomide in rheumatoid arthritis. *Clin. Immunol.* **1999**, *93*, 198–208.
- (13) Peters, G. J.; Sharma, S. L.; Laurensse, E.; Pinedo, H. M. Inhibition of pyrimidine de novo synthesis by DUP-785 (NSC 368390). *Invest. New Drugs* **1987**, *5*, 235–244.
- (14) Leban, J.; Saeb, W.; Garcia, G.; Baumgartner, R.; Kramer, B. Discovery of a novel series of DHODH inhibitors by a docking procedure and QSAR refinement. *Bioorg. Med. Chem. Lett.* **2004**, *14*, 55–58.
- (15) Leban, J.; Kralik, M.; Mies, J.; Gassen, M.; Tentschert, K.; Baumgartner, R. SAR, species specificity, and cellular activity of cyclopentene dicarboxylic acid amides as DHODH inhibitors. *Bioorg. Med. Chem. Lett.* **2005**, *15*, 4854–4857.
- (16) Baumgartner, R.; Walloschek, M.; Kralik, M.; Gotschlich, A.; Tasler, S.; Mies, J.; Leban, J. Dual binding mode of a novel series of DHODH inhibitors. *J. Med. Chem.* **2006**, *49*, 1239–1247.
- (17) Hurt, D. E.; Sutton, A. E.; Clardy, J. Brequinar derivatives and species-specific drug design for dihydroorotate dehydrogenase. *Bioorg. Med. Chem. Lett.* **2006**, *16*, 1610–1615.
- (18) Kremmer, J. M. What I would like to know about leflunomide. *J. Rheumatol.* **2004**, *31*, 1029–1031.
- (19) Payne, D. J.; Gwynn, M. N.; Holmes, D. J.; Pompliano, D. L. Drugs for bad bugs: Confronting the challenges of antibacterial discovery. *Nat. Rev. Drug Discovery* **2007**, *6*, 29–40.
- (20) Bostock, J. M.; Chopra, I.; Johnson, A. P.; Hesse, L.; Horton, J. R.; Fishwick, C. W. G. Macrocyclic Inhibitors of the Bacterial Cell Wall Enzyme MurD. *Bioorg. Med. Chem. Lett.* **2003**, *13*, 1557–1560. Ali, M. A.; Bhogal, N.; Findlay, J. B. C.; Fishwick, C. W. G. The first de novo designed antagonists of the human NK2 receptor. *J. Med. Chem.* **2005**, *48*, 5655–5658. Besong, G. E.; Bostock, J. M.; Stubbings, W.;

- Chopra, I.; Roper, D. I.; Lloyd, A. J.; Fishwick, C. W. G.; Johnson, A. P. A novel de novo designed inhibitor of D-Ala-D-Ala ligase from *E. coli*. *Angew. Chem., Int. Ed.* **2005**, *44*, 6403–6406.
- (21) Heikkila, T.; Thirumalairajan, S.; Davies, M.; Parsons, M. R.; McConkey, G. A.; Fishwick, C. W. G.; Johnson, A. P. The first de novo designed inhibitors of *Plasmodium falciparum* dihydroorotate dehydrogenase. *Bioorg. Med. Chem. Lett.* **2006**, *16*, 88–92.
- (22) Kuo, E. A.; Hambleton, A. B.; Kay, D. P.; Evans, P. L.; Matharu, S. S.; Little, E.; McDowall, N.; Jones, C. B.; Hedgecock, C. J. R.; Yea, C. M.; Chan, A. W. E.; Hairsine, P. W.; Ager, I. R.; Tully, W. R.; Williamson, R. A.; Westwood, R. J. Synthesis, structure-activity relationships, and pharmacokinetic properties of dihydroorotate dehydrogenase inhibitors: 2-Cyano-3-cyclopropyl-3-hydroxy-N-[3'-methyl-4'-(trifluoromethyl)phenyl]propenamide and related compounds. *J. Med. Chem.* **1996**, *39*, 4608–4621.
- (23) Phillips, M. A.; Gujjar, R.; Malmquist, N. A.; White, J.; El Mazouni, F.; Baldwin, J.; Rathod, P. K. Triazolopyrimidine-based dihydroorotate dehydrogenase inhibitors with potent and selective activity against the malaria parasite *Plasmodium falciparum*. *J. Med. Chem.* **2008**, *51*, 3649–3653.
- (24) Patel, V.; Booker, M.; Kramer, M.; Ross, L.; Celatka, C. A.; Kennedy, L. M.; Dvorin, J. D.; Duraisingh, M. T.; Sliz, P.; Wirth, D. F.; Clardy, J. Identification and Characterization of Small Molecule Inhibitors of *Plasmodium falciparum* Dihydroorotate Dehydrogenase. *J. Biol. Chem.* **2008**, *283*, 35078–35085.
- (25) Kuo, P. Y.; Shie, T. L.; Chen, Y. S.; Lai, J. T.; Yang, D. Y. Enzyme inhibition potency enhancement by active site metal chelating and hydrogen bonding induced conformation-restricted cyclopropanecarbonyl derivatives. *Bioorg. Med. Chem. Lett.* **2006**, *16*, 6024–6027.
- (26) Baldwin, J.; Michnoff, C. H.; Malmquist, N. A.; White, J.; Roth, M. G.; Rathod, P. K.; Phillips, M. A. High-throughput screening for potent and selective inhibitors of *Plasmodium falciparum* dihydroorotate dehydrogenase. *J. Biol. Chem.* **2005**, *280*, 21847–21853.
- (27) Heikkila, T.; Ramsey, C.; Davies, M.; Galtier, C.; Stead, A. M. W.; Johnson, A. P.; Fishwick, C. W. G.; Boa, A. N.; McConkey, G. A. Design and synthesis of potent inhibitors of the malaria parasite dihydroorotate dehydrogenase. *J. Med. Chem.* **2007**, *50*, 186–191.
- (28) Malmquist, N. A.; Gujjar, R.; Rathod, P. K.; Phillips, M. A. Analysis of flavin oxidation and electron-transfer inhibition in *Plasmodium falciparum* dihydroorotate dehydrogenase. *Biochemistry* **2008**, *47*, 2466–2475.
- (29) Clarke, D.; Ali, M. A.; Clifford, A. A.; Parratt, A.; Rose, P.; Schwinn, D.; Bannwarth, W.; Rayner, C. M. Reactions in unusual media. *Curr. Top. Med. Chem.* **2004**, *4*, 729–771.

JM800963T